CCUS: 4015303

Enhancing Oil Recovery in Heterogeneous Reservoirs with CO_2 Flooding: A Simulation Study

Hossam Ebaid*[1], Moamen Gasser[1], Taha Yehia[1], Esuru R. Okoroafor[1]
1. Texas A&M University.

Abstract

This study examines challenges in CO_2-EOR, like small-scale reservoir factors, viscous and interfacial forces, and dispersive effects due to concentration gradient, focusing on how these small-scale reservoir parameters impact oil recovery during CO_2 injection.

A suite of simulation models representing various heterogeneity patterns was developed, and these models were subjected to differing pressures, both above and below the Minimum Miscibility Pressure (MMP). A simple 2D reservoir model was built as a compositional oil model using Eclipse 300. It consists of 100 cells in the x-direction and 20 cells in the z-direction, totaling 2000 cells. To simulate injection and production into the model, two vertical wells were placed at either end of the model, fully penetrating the z-direction. This allows the CO_2 to sweep the oil from the injector to the producer.

After conducting 21 model simulations, the study revealed that below the Minimum Miscibility Pressure (MMP), gravitational effects were the primary driving force, causing gas to override oil, with permeability playing a minor role. Above the MMP, viscous forces induced fingering and early breakthrough. All models showed improved oil recovery due to miscibility, with the k_v/k_h ratio being a crucial factor. Coarsening of horizontal permeability, or both horizontal and vertical permeabilities, had a detrimental impact on recovery. Gas override was influenced by both horizontal and vertical permeability, leading to fingering under random permeability distributions. Horizontal permeability variations, regardless of vertical permeability consistency, had the most significant impact on oil recovery. Additionally, the study emphasized that the coefficient of variation (Cv) alone inadequately characterized heterogeneity, as models with the same Cv values exhibited varying recovery outcomes, ranging from 63% to 96.5%.

The novelty of this study is that it quantifies the impact of heterogeneity on CO_2 EOR recovery. These findings underscore the intricate relationship between reservoir parameters and CO_2 miscible flooding, offering essential insights for optimizing EOR strategies in heterogeneous reservoirs.

1. Introduction

Over the last few decades, the amount of oil produced has increased rapidly due to the increase in oil consumption worldwide (Bello et al. 2023). To meet the world's need for energy, several techniques are used to increase oil recovery from mature or depleted fields (Leonhard Ganzer et al. 2017). After primary recovery using the natural energy of the reservoir and secondary recovery using water flooding, a large amount of oil remains trapped in the narrow pores of the reservoir rocks. Enhanced Oil Recovery (EOR) methods have been used for decades to improve oil recovery and decrease residual oil saturation remaining in the reservoir (Bello et al. 2023).. The main objective of EOR methods is to achieve a favorable mobility ratio between the two fluids thus improving sweep efficiency or changing the interfacial forces or capillary pressure (Xiao Deng et al. 2020). EOR is thus believed to be one of the most important areas of technology in the petroleum industry (Mostafa Iravani, et al. 2023).

EOR methods can be classified into the following areas: chemical, thermal, and miscible methods (Alvarado and Manrique 2010). Some chemical methods include, polymer flooding, alkaline flooding, and surfactant flooding (Ragab and Mansour 2021; Razman Shah et al. 2023). These methods enhance oil recovery by adding certain chemicals to the water to change the viscosity or create interfacial conditions that produce a favorable mobility ratio (Pashapouryeganeh et al. 2022). Thermal methods include cyclic steam injection, steam drive, and in-situ combustion (Antolinez et al. 2023). These methods enhance oil recovery using heat to reduce the oil's viscosity (Pan et al. 2023). Heat can also vaporize some of the light components into the gas phase. Therefore, the oil is lighter and can easily be displaced (Zhao et al. 2020; 2021). Miscible methods include displacement using Liquefied Petroleum Gas (LPG), Nitrogen, or Carbon dioxide (CO_2). Miscible displacement was defined as "*the displacement of oil by fluids with which it mixes in all proportions without the presence of an interface*" (Carcoana 1992).

CO_2 emerges as a powerful tool in EOR applications due to its unique miscibility properties. Thus, CO_2-EOR presents a win-win scenario for both energy production and environmental sustainability, making it a crucial technology for maximizing resource utilization and minimizing emissions in the oil and gas industry (Fahad I. Syed et al. 2022). In mature oilfields, conventional extraction methods leave significant oil trapped within the reservoir (Zhengxiao Xu et al. 2020). Injecting supercritical CO_2 into these formations unlocks this trapped resource through several mechanisms (Jin et al. 2017). Firstly, CO_2 dissolves oil components, causing swelling and viscosity reduction, which facilitates flow towards production wells. This "miscible displacement" maximizes oil recovery compared to water flooding. Secondly, CO_2 interacts with rock minerals, altering wettability and favoring oil release. Moreover, CO_2-EOR offers additional benefits: it can act as a geological storage site for captured CO_2, mitigating greenhouse gas emissions, and its utilization creates economic value from depleted fields (Abubakar Isah et al. 2022).

The implementation of CO_2-EOR in mature oilfields is accompanied by challenges that may undermine project viability(Pimenta et al. 2022). These challenges encompass small-scale reservoir factors, viscous forces, interfacial forces governing fluid behavior in the reservoir, and dispersive forces resulting from concentration gradients among fluids (Mohamad Yousef Alklih et al. 2021). A pivotal determinant influencing reservoir performance during CO_2 flooding is reservoir heterogeneity, defined as the spatial variability of rock properties, including porosity, permeability, facies, and thickness (Ahmed 2006). Reservoir heterogeneities can precipitate premature CO_2 breakthrough, inducing channeling and dispersion phenomena. Consequently, these issues may lead to inadequate oil displacement, rendering the overall CO_2-EOR project economically unfeasible. Mitigating such challenges necessitates meticulous reservoir characterization, utilization of advanced modeling techniques, and comprehensive risk assessments(Muataz Alshuaibi et al. 2018). Engineers and geoscientists engaged in CO_2-EOR endeavors must account for reservoir heterogeneity's impact on fluid flow and displacement efficiency (Mohamad Yousef Alklih et al. 2019). Strategic adjustments to injection methodologies, well placement, and operational parameters may be requisite to address identified challenges. Ongoing technological advancements and continuous research in enhanced oil recovery contribute to refining the understanding and application of CO_2-EOR techniques, particularly in the context of mature oilfields(Seyedeh Hosna Talebian et al. 2014).

The main objective of this research is to study the effect of small-scale reservoir factors on oil recovery using CO_2 injection. This involves reproducing the slim tube experiments presented by Holms and Josendal using very fine-scale simulation models (Holm and Josendal 1974). Provided that the pressure is high enough, it is known that CO_2 is miscible with oil in a 1D model (slim tube experiment). However, reservoir

rocks are complex and heterogeneous, and we have flow in 3D. It is not yet understood whether the miscibility effects will be insignificant in a heterogeneous model, or if they will be enhanced. Also, if there is a gravity override, the CO_2 could bypass the oil, and hardly mix with it at all. So, the aim is to determine what effects are important. Therefore, various models have been constructed with different static model heterogeneities. Sensitivity analysis on the effect of reservoir heterogeneities effect on gas miscibility, oil recovery and the effect of coefficient of variation on oil recovery have been investigated.

2. Methodology

2.1. Base Case Description

To study the effect of fine-scale geological structures on CO_2-EOR, a simple 3D grid model was built using Eclipse reservoir simulator (E-300). The model dimensions are 10m by 1m by 2m consisting of 2000 cells each is 0.1m by 0.1m by 0.1m and divided as 100 cells in the x-direction and 20 cells in the z-direction. The base case model is a compositional oil model with homogeneous rock properties as summarized in Table A.1 in Appendix A. Initially, the fluid properties such as density and formation volume factors were estimated using the Peng-Robinson equation of state based on a seven-component reservoir fluid as shown in Table A.2 while Table A.3 shows the oil-gas relative permeability curves. To simulate injection and production into the model, two vertical wells were placed; an injector in grid cell (1, 1) and a producer in grid cell (100, 1). Both wells were completed in all layers so that injection and production happened in all 20 layers to allow the CO_2 to sweep the oil from the injector to the producer. The producer was modeled to produce at a minimum Bottom Hole Pressure (BHP) equal to the reservoir pressure (i.e., 50 bar). Later, the pressure increased to above the minimum miscibility pressure (MMP). The injector was modeled to inject 1.2 of the pore volume (PV) at a rate of 0.48 m3/day for 12 hours. Figure 1 shows the initial gas saturation in the model.

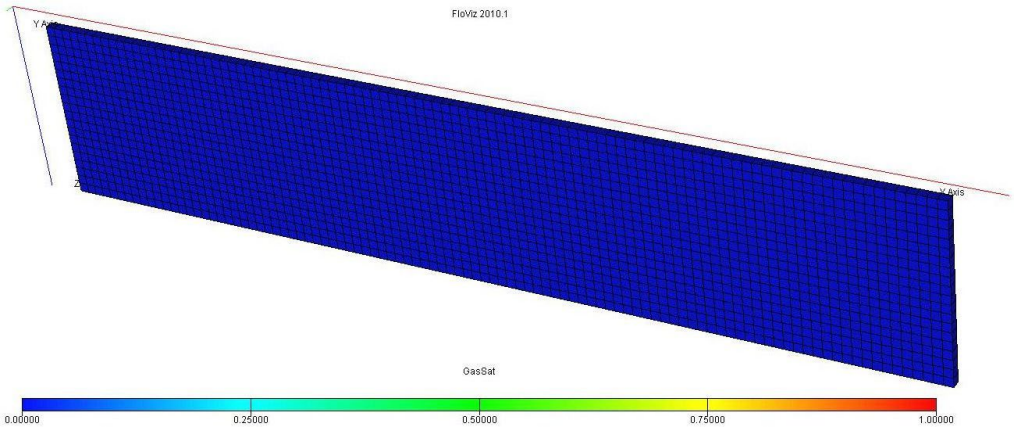

Figure 1. shows the initial gas saturation of the base case model (i.e., Model 1).

2.2. Scenarios Investigated

Different scenarios were created to study the effect of heterogeneity, each with a different distribution of permeabilities among the layers. Each scenario was run at different reservoir pressures between 50 bars and 300 bars. After that, 1.2 PV was injected and the recovery was plotted against pressure to determine the MMP. Moreover, the gas saturation in the model was observed at pressures above and below the MMP. For each case, the coefficient of variation was calculated, and oil recovery was compared to the homogeneous base case, initially, named Model 1 which has identical horizontal and vertical permeabilities each equal to 500mD.

To investigate the effect of anisotropy on CO2 recovery, Model 2 to Model 4 were homogeneous but had different k_v/k_h ratios. Only the horizontal permeability was changing while the vertical permeability was kept constant. These values are constant for all cells in a single model but differ from one model to another. For these 3 models, the k_v/k_h ratios are greater than 1 although it is usually uncommon unless fissures or natural fractures exist in the horizontal direction. On the other hand, Model 5 to Model 7 were created to investigate the effect of changing the vertical permeability and keeping the horizontal permeability constant.

It should be noted that for these first 6 models, the value for permeability is constant for all cells in a model but changes from one model to another.

In another scenario, the horizontal permeability of Model 8 was made to coarsen upward with each layer while the vertical one was kept constant. On the contrary, the vertical permeability in Model 9 was made to coarsen upward with each layer while the horizontal one was kept constant. Finally, both horizontal and vertical permeability of Model 10 were made to coarsen upward together so that each layer in the model is isotropic.

To investigate the effect of fining upwards on CO_2-EOR, Models 11 to 13 were created in which the grains get smaller with height and the permeability is larger at the bottom of the model than at the top. Also, the effect of layering on CO_2 recovery was investigated by making each model have layers with high and low permeability. For example, Model 14 was constructed to have layers of 500mD and 100mD while Model 15 was constructed to have layers of 500 mD and 250 mD.

In another scenario, the horizontal permeability of Model 16 was made to vary randomly from layer to layer while the vertical one was kept constant. Contrary, the vertical permeability of Model 17, was made to vary randomly while the horizontal one was kept constant. Finally, the effect of different values of horizontal permeabilities was investigated. These values were randomly distributed amongst the layers while the vertical permeability was kept constant in Model 19. Similarly in Model 20, the same permeability values were used but permeability was made to vary both horizontally and vertically. For Model 21 and Model 22, the permeability was randomly distributed among the different layers too. However, the layers themselves were isotropic (i.e. the horizontal and vertical permeability are equal). Table 1 summarizes the permeability distributions of all cases in this study.

Table 1. summarizes the permeability distributions of all cases in this study.

Model No.	**Horizontal Permeability Kh**	**Vertical permeability K_v**	**K_v/K_h ratio**	**Comments**
1	500	500	1	Homogeneous
2	125	500	4	Homogeneous
3	250	500	2	Homogeneous
4	375	500	1.333	Homogeneous
5	500	125	0.25	Homogeneous
6	500	250	0.5	Homogeneous
7	500	375	0.75	Homogeneous
8	coarsening upward	500		
9	500	coarsening upward		
10	coarsening upward	coarsening upward		
11	fining upwards	500		
12	500	fining upwards		
13	fining upwards	fining upwards		
14	alternating layers of 500 and 100 mD	alternating layers of 500 and 100 mD		
15	alternating layers of 500 and 250 mD	alternating layers of 500 and 250 mD		
16	Random	500		
17	500	random		
18	Random	500		
19	Random	random		Isotropic
20	Random	random		Isotropic
21	Random	random		Isotropic

3. Results and Discussion

3.1. Investigation of Minimum Miscibility Pressure (MMP)

The first step was to find MMP by running Models 2-14 at different pressures. The recovery was then plotted after 12 hours of injection of 1.2 PV versus pressure on a cartesian scale. Models 2-4 show the effect of changing the horizontal permeability of the whole model to be less than the vertical permeability of the model. As the pressure increases, the recovery increases until a pressure of about 175 bars where the recovery becomes constant. This is taken to be the MMP. Also, when comparing these 3 models to Model 1 (i.e., base case model), it showed the same trend and same MMP meaning that K_v/K_h ratio above 1 has no effect on recovery or MMP as shown in Figure 2.a. Meanwhile, Models 5-7 show the effect of changing the vertical permeability of the whole model making it less than the horizontal permeability and thus the kv/kh ratio is less than 1. It could be seen that as the pressure increases, the recovery increases until a pressure of also about 175 bars where the recovery plateaus as shown in Figure 2.b. This again confirms the MMP of 175 bars. Although the MMP is the same, the models have different recoveries. It is seen that as the vertical permeability decreases the recovery increases. This is because there is less crossflow, so flow is directed in the horizontal direction, leading to a better sweep efficiency and higher recovery.

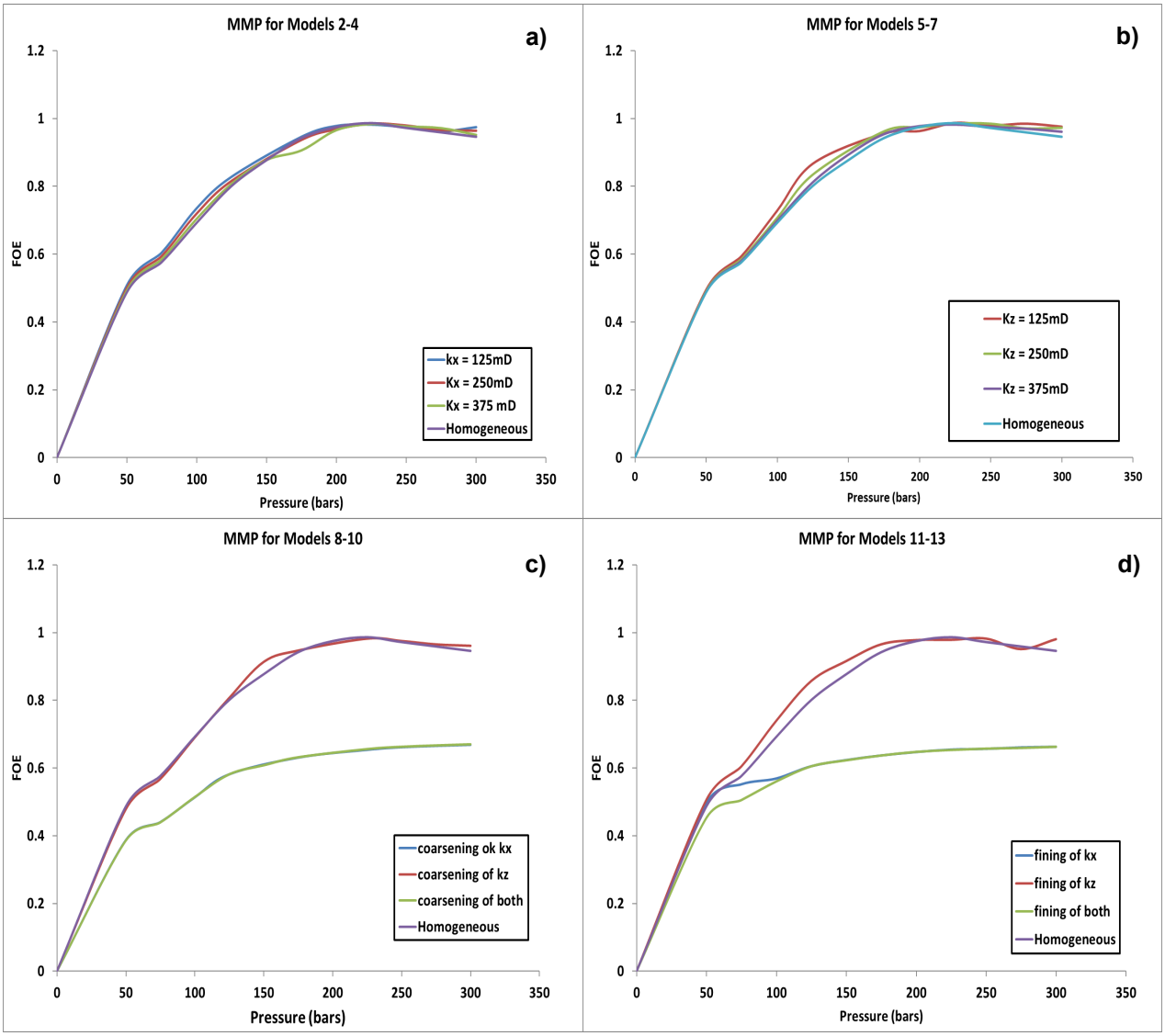

Figure 2. Shows the recovery versus pressure for a) Models 2-4, b) Models 5-8, c) Models 9-11, and d) Models 12-14.

Moreover, Models 8-10 show the effect of coarsening upward of horizontal permeability, vertical permeability, and both at the same time. For Models 8 and 10, both show the same trend for increase the recovery versus pressure and show a MMP between 150 bars and 200 bars. The abovementioned models also show a reduction in recovery compared to the Model 1 and Model 9 because the horizontal permeability is higher at the top of the model than at the bottom. While the vertical permeability is kept constant at 500mD, cross flow is much higher and so flow is diverted into the top layers and oil is bypassed leading to early breakthrough. Model 9 shows higher recovery compared to Models 8 and 10 because the vertical permeability is higher at the top of Model 9 than at the bottom while the horizontal permeability is kept constant at 500mD as shown in Figure 2.c. This leads to less cross flow due to lower permeability; therefore, the flow is better in the horizontal direction, leading to better oil sweeping. For all models the MMP is again between 150 bars and 200 bars and is also taken to be 175 bars.

Furthermore, Models 12-14 show the effect of fining upward of horizontal permeability, vertical permeability, and both simultaneously. Fining upward means that the permeability at the top of the model is lower than the permeability at the bottom of the model. For Model 12, the recovery is very high and very similar to the homogeneous case. This is because for this case, the vertical permeability is lower at the top of the model and the horizontal permeability is kept constant at 500mD the cross flow is much lower at the top and so flow is confined to the top layers and oil is swept from these layers. This is also aided by gravity which helps the gas flow upward which caused most the layers to be swept. On the other hand, Model 11 where fining is of horizontal permeability only and vertical permeability is kept constant at 500mD, the recovery was found to be much lower as shown in Figure 2.d. This is because vertical permeability is much higher than horizontal permeability and so cross flow occurs, and flow is diverted into lower layers only keeping the top layers unswept. The same occurs with Model 13 since both horizontal and vertical permeability are both fining so flow is diverted into lower layers with higher permeability.

3.2. Effect of heterogeneity on gas saturation

The following figures show the gas saturation in each model after 6 hours of injection time. The models were analyzed at two pressures of 100 bars, and 250 bars, to see the effect before and after miscibility is achieved. Figure 3 shows the gas saturation in the homogeneous model from a pressure of 100 bars to 250 bars in Models 1. It is seen that below miscibility the flow is gravity dominated and the gas rises due to low density and overrides. As the miscibility pressure is reached, the degree of override decreases until it reaches an almost constant front at a pressure of 250 bars. Figure 4 shows the gas saturation after six hours of gas injection into Model 3. It is seen that below the miscibility pressure, the gas tends to be gravity dominated again and rises due to its low density compared to the oil. However, as the MMP is reached, the two fluids become miscible and their densities are closer together, resulting in a decreased degree of gas override.

In addition, the degree of override decreases as the horizontal permeability decreases. Asis is because as the horizontal permeability decreases, the pressure in the injector increases since we are injecting at the same rate. This means that the flood becomes more miscible as the pressure increases, and as the permeability decreases. Comparing Figure 4 to Figure 3, we see that there is no fingering at the top of the model as with the homogeneous and a more even distribution of gas. The same phenomenon is seen with Models 2 and 4. Figure **5** shows the gas saturation for Model 6 for the same 2 pressures. Again, the same phenomenon is observed, and gas is seen to rise due to gravity at pressures lower than the miscibility pressure. This degree of override decreases with increasing pressure until the front is almost constant. It can be observed that as the vertical permeability decreases the gas override decreases until it reaches a constant front as in the case where there is no cross flow.

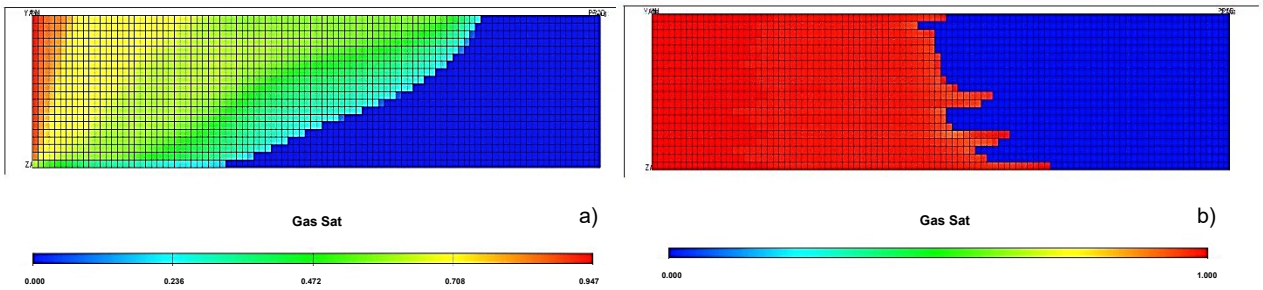

Figure 3. Shows gas saturation in Model 1 at a) 100 bars and b) 250 bars.

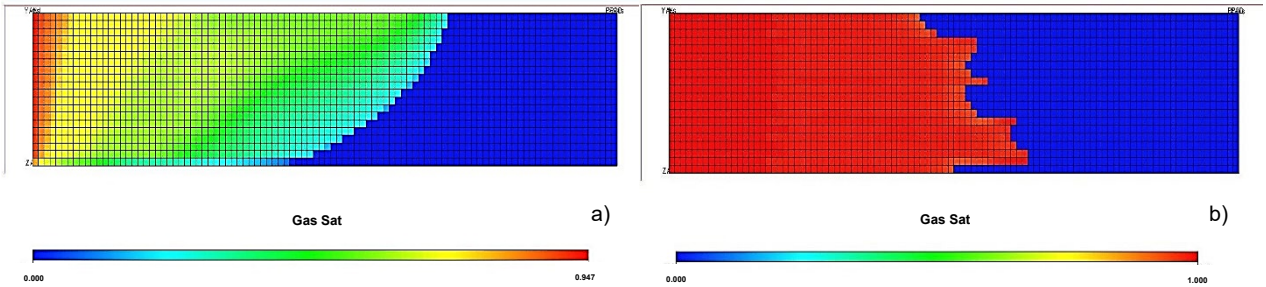

Figure 4. Shows gas saturation in Model 3 at a) 100 bars and b) 250 bars.

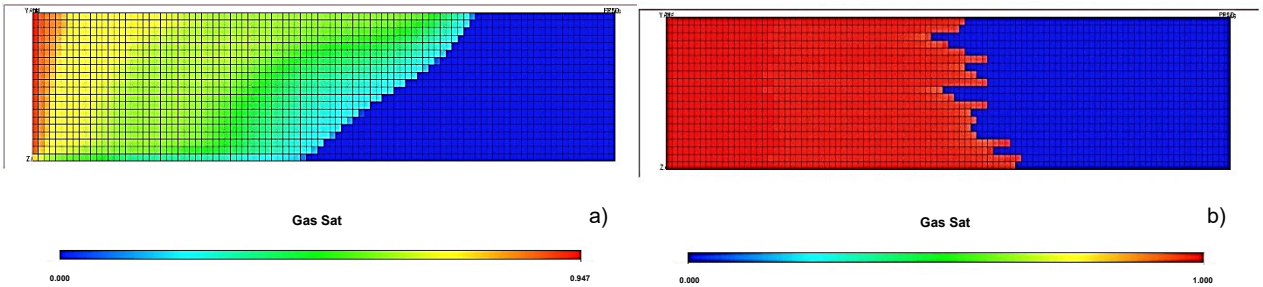

Figure 5. Shows gas saturation in Model 6 at a) 100 bars and b) 250 bars.

Furthermore, gas override in Model 8 is large due to the tendency of gas to rise, as it has small density. This is aided by the very high vertical permeability causing the gas to rise even more. This causes the layers at the top of the model to have almost 100% gas saturation compared to almost 0% at the bottom of the model. This occurs at all pressures but is greater at pressures lower than MMP. Figure 6 shows the gas saturation for Model 8 at 100 bars, and 250 bars respectively. Figure 7 shows the gas saturation for model 10 where both horizontal and vertical permeability is coarsening upward. It is clear that gas overrides again due to the low overall permeability at the base of the model compared to the permeability at the base of the model. This is also aided by the low gas density, forcing it to increase. This is the same at all pressures. However, it is greater at lower pressures. Figure 8 shows the gas saturation after 6 hours of gas injection for Model 12 where the horizontal permeability is fining upward. This means that horizontal permeability is lower at the top of the model than at the bottom. This causes the gas to slump downward. Although gas tends to go up, the very low horizontal permeability renders flow in this direction and flow is forced to move down since the vertical permeability is much higher. At pressures below the MMP the gas saturation covers more layers in the model than at higher pressures because the flow is gravity-dominated, and gas is trying to override but is stopped by the very low permeability at the top. However, at Pressure equal to or greater than MMP the gas is viscous-dominated and flows through the high permeability layers.

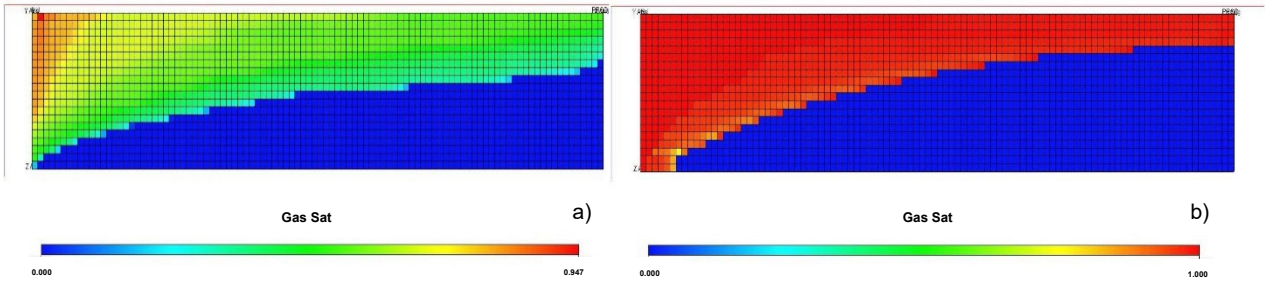

Figure 6. Shows gas saturation in Model 8 at a) 100 bars and b) 250 bars.

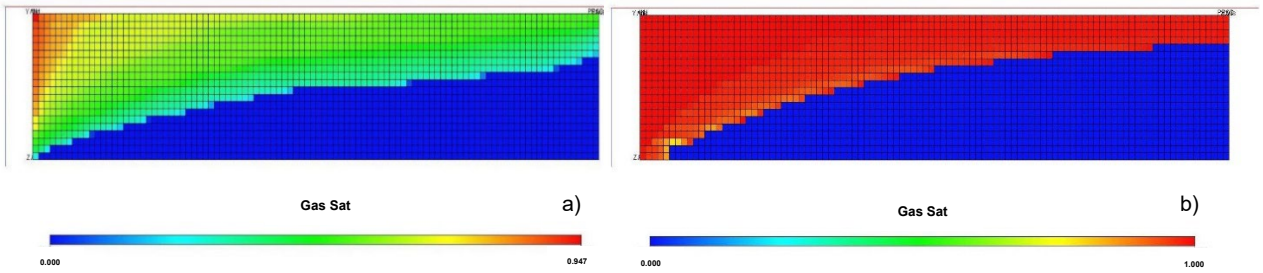

Figure 7. Shows gas saturation in Model 10 at a) 100 bars and b) 250 bars.

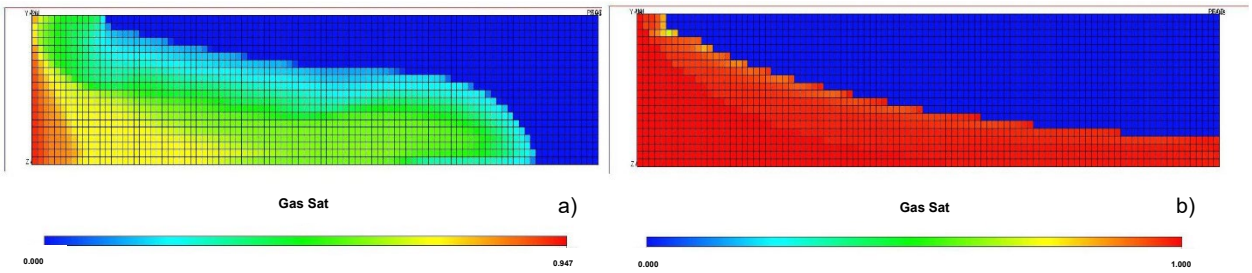

Figure 8. Shows gas saturation in Model 12 at a) 100 bars and b) 250 bars.

In Model 14, it has been observed that gas is forced down since permeability is higher at the base of the model than at the top. Figure 9 shows the gas saturation for Model 14 where both the horizontal and vertical permeability are fining upward. Below the MMP the gas saturation covers a large area of the model, this is because the gas is trying to move upward due to its density. At higher pressures the flow is no longer gravity dominated and flows through the passage of high permeability and moves to the lower layers more quickly. Figure 10 shows the gas saturation in Model 15. This model has homogeneous layers of alternating permeability of 500mD and 100mD. It is seen that pressures below the MMP layering have no effect on the gas saturation profile, and the gas tends to override, and breakthrough occurs at the top layers first. The flow is gravity dominated. At MMP the flow is viscous dominated and gas flows through the high permeability layers first and the saturation is almost 100% in these layers and very low in the low permeability layers causing a fingering effect. Figure 11 shows the gas saturation in Model 16 below, at and above the MMP. Here again the same phenomenon as Model 15 is observed but the gas saturation in the lower permeability layers is higher since the permeability values are closer together than in Model 14.

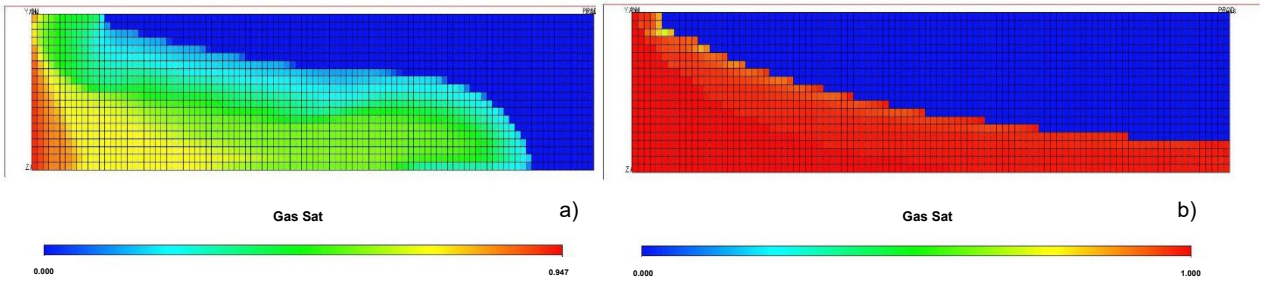

Figure 9. Shows gas saturation in Model 14 at a) 100 bars and b) 250 bars.

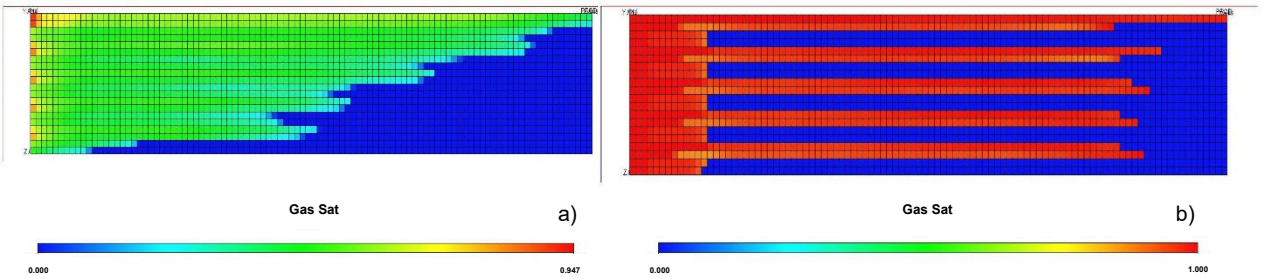

Figure 10. Shows gas saturation in Model 15 at a) 100 bars and b) 250 bars.

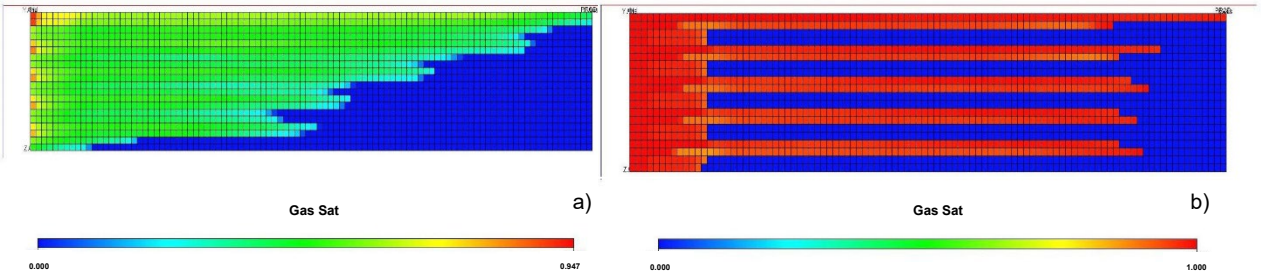

Figure 11. Shows gas saturation in Model 16 at a) 100 bars and b) 250 bars.

In Model 17, at 100 bars the gas saturation covers the whole model and has an almost piston like displacement. Figure 12 shows the gas saturation in Model 17 where the horizontal permeability was randomly distributed to each layer and the vertical permeability is kept constant at 500mD. This is because the horizontal permeability is lowered, and vertical permeability is constant and so gas moves upward due to its low density however it cannot move in the horizontal direction. At MMP the gas override does not exist, and flow is once again viscous dominated, and flow occurs through the high permeability layers and not through others. This leads to fingering and early breakthrough in the high permeability layers. Figure 13 shows the gas saturation for Model 19. In this model the horizontal permeability was made to vary randomly with depth and vertical permeability kept constant at 500mD. At 100 bars the gas is gravity dominated and moves upward due to density. The gas tends to override, and breakthrough occurs at the top layers. At higher pressures the gas no longer overrides and moves through the layers of high permeability first causing fingering. Breakthrough occurs in these layers first. Figure 14 shows the saturation for Model 20. Model 20 has the same permeability values as Model 19, but this time permeability varies in both the horizontal and vertical direction. It is seen that at the lower pressures, the gas override is not seen as in Model 19 since there are some very low permeability layers in the vertical direction preventing cross flow. At MMP and above, the effect is the same as in Model 19, and the flow is viscous-dominated and moves through the high permeability layers faster.

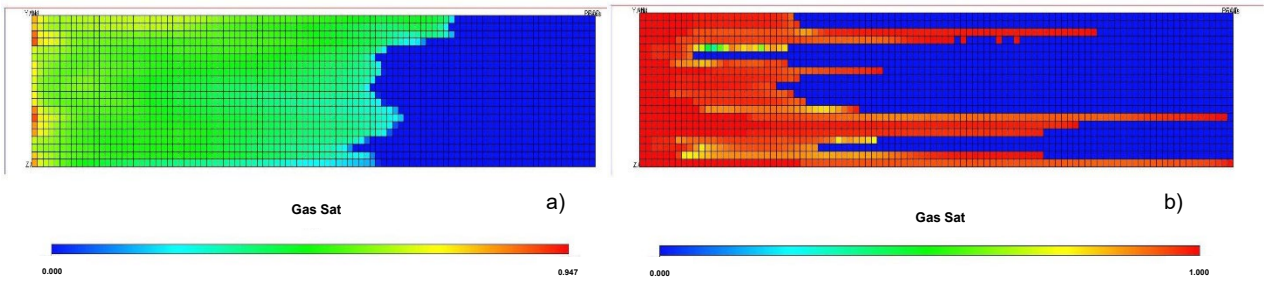

Figure 12. Shows gas saturation in Model 17 at a) 100 bars and b) 250 bars.

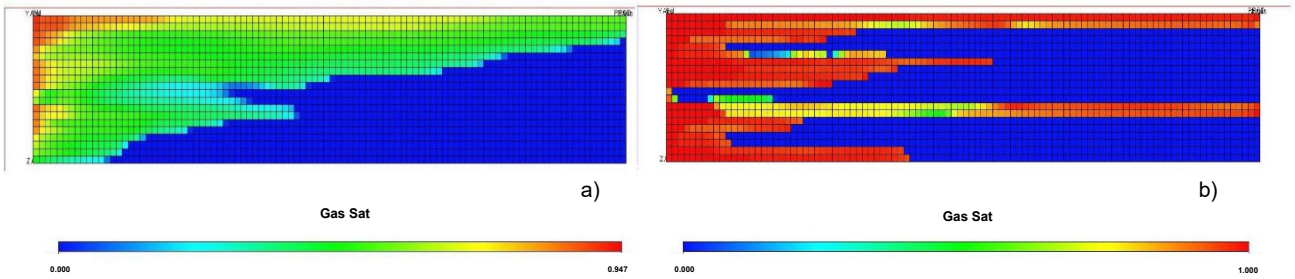

Figure 13. Shows gas saturation in Model 19 at a) 100 bars and b) 250 bars.

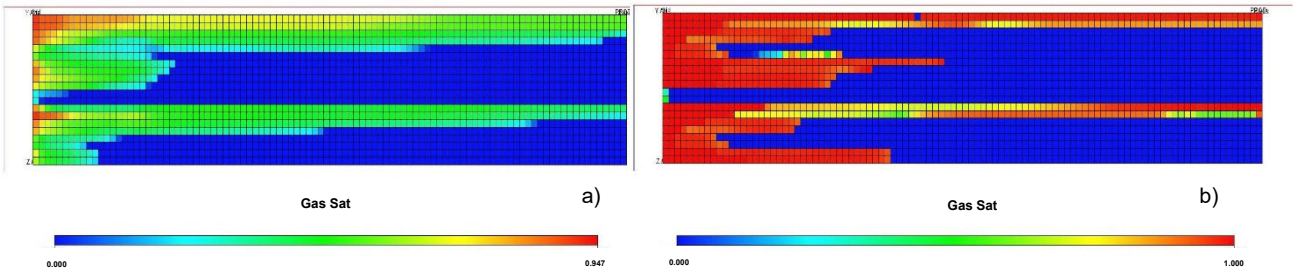

Figure 14. Shows gas saturation in Model 20 at a) 100 bars and b) 250 bars.

3.3. Effect of Heterogeneity on Oil Recovery

It has been clear till now that reservoir heterogeneity and small-scale reservoir structures affect the gas saturation in the reservoir and would therefore affect the overall oil recovery. **Table 2** summarizes the oil recovery from each of the 22 models outlined earlier. The recovery after injection of 1.2PV of CO_2 is recorded at the MMP and before MMP. The increase in recovery due to miscibility is also calculated. Also, the table includes the coefficient of variation for each case as a measure of the degree of heterogeneity.

We can see that for the first 8 eight models, the recovery at MMP is almost the same as the homogeneous. Models 2-4 where the horizontal permeability was reduced showed the same recovery as the homogeneous model at MMP. However, Models 5-7 where the vertical permeability was reduced show slight increase (+1-2%) in recovery. These 7 models have a coefficient of variation of zero since all the layers have the same value of permeability and so the layers are basically all homogeneous but with different k_v/k_h ratio making them anisotropic. Below MMP these 7 models show drastically lower recoveries, with an increase in recovery of about 22% due to miscibility.

It is noticed that Model 9 also has a very high recovery compared to Models 8 and 10 at the MMP. For Model 9 the vertical permeability was coarsening upward while the horizontal permeability was kept constant and so cross flow was less at the bottom of the model and higher at the top leading to higher recovery. Models 8 and 10 have a much lower recovery of 63.1%. In these two models, horizontal permeability was made to coarsen upward showing that it deeply affected recovery. Below MMP the recovery shows the same trend, however recoveries are much lower. For Model 9, there is a 25% increase in recovery due to miscibility, whereas for Models 8 and 10 there is only an 11% increase.

Table 2. Summary of Cv and oil recovery for each model

Model no.	Coefficient of variation (Cv)	Overall Oil Recovery (%) at MMP (175 bars)	Overall Oil Recovery (%) at 100 bars	Increase in oil Recovery due to miscibility (%)
1	0	94	69.2	24.8
2	0	94.6	73.6	21
3	0	93.6	72	21.6
4	0	94.4	70.4	24
5	0	95.6	72.8	22.8
6	0	96.2	70.7	25.5
7	0	95.4	69.9	25.5
8	0.44	63.1	51.4	11.7
9	0.44	94.7	69	25.7
10	0.44	63.1	51.4	11.7
11	0.44	63.6	56.9	6.7
12	0.44	96.5	74	22.5
13	0.44	63.8	56.1	7.7
14	0.56	84.5	51.6	32.9
15	0.28	70	55.2	14.8
16	0.54	76.3	59.3	17
17	0.54	95.7	59.6	36.1
18	0.79	70.7	56.6	14.1
19	0.79	61.5	47.2	14.3
20	0.65	65.5	59.2	6.3
21	0.34	77.6	68.4	9.2

Model 12 was also found to have a recovery of 96.5% compared to 63.6% and 63.8% for Models 11 and 13. This is because Model 12 has vertical permeability fining upward while the horizontal permeability is kept constant. On the other hand, Model 11 has horizontal permeability fining upward and vertical permeability constant while model 13 has both fining upward. At a pressure of 100 bars, the recovery has the same trend but lower. Moreover, the recovery of Model 12 increased by 22% due to miscibility while for Models 11 and 13 there was only 7% increasement.

Models 14 and 15 are for alternating layers of high and low permeability. Model 14 has a recovery of 84.5% compared to Model 15 which only has a recovery of 70%. This is because Model 14 shows higher permeability contrast since the layers have permeability of 500mD and 100mD compared to Model 15 which has permeability of 500mD and 250mD, Model 14 has Cv of 0.56 compared to 0.28 for Model 15. The reason behind this larger recovery is that because the layers have the same value of permeability in the vertical direction as the horizontal direction, flow in the vertical direction is less in these layers and so gas cross flow is less and sweeps more in the horizontal direction. Model 14 also shows a higher increase in recovery (32.9%) due to miscibility compared to Model 15 which only shows a 14.8% increase.

Models 16 and 17 are for models where the permeability was random in the horizontal and vertical direction respectively. Model 16 shows a much lower recovery of 76.3% compared to Model 17 which has a recovery of 95.7%. Again, changing the horizontal permeability and keeping the vertical permeability

constant reduced recovery compared to the case where the horizontal was constant. This gave way to more gas override and so oil is bypassed and less recovery. This again is the same for pressure below MMP.

Model 18 has a recovery of 70.5 % compared to 61.7 % for Model 19. These two models also investigated the effect of random permeability, however model 18 had random horizontal permeability and constant vertical permeability which led to higher recovery than model 19 where both the horizontal and vertical permeability were both random. Both models showed an increase in recovery of about 14% due to miscibility.

It is also seen that Models 20 and 21 have different recoveries of 65.5% and 77.6 % respectively. Although both models have random permeability in both the horizontal and vertical direction, both models have different values of permeability given by the different Cv values (0.65 for model 20 compared to 0.34 for model 21). Model 21, being more homogeneous than Model 20 shows a higher recovery. However, the increase in recovery for these two models due to miscibility is not great with only 6.3% increase in Models 20 and 9.2 % increase in Model 21.

3.4. Effect of Coefficient of Variation on Recovery

To investigate if a relation exists between Cv and recovery, a comparison is made between the different models. However, to be able to compare we must group the models together according to the direction in which the permeability is changing. This section examines the effect of changing the horizontal permeability only, changing the vertical permeability only and then changing both at the same time. For example, Table 3 shows the recovery at 175 bars and Cv for the models in which the horizontal permeability was made to vary, and vertical permeability was made constant at 500mD.

Table 3. Oil recovery for variation in horizontal permeability

Model	Cv	Oil Recovery
8	0.44	63.1
11	0.44	63.6
16	0.54	76.3
18	0.79	70.7

Moreover, Table 4. shows the recovery and Cv for the models in which vertical permeability was made to vary and horizontal permeability was made constant at 500mD.

Table 4. Oil recovery for variation in vertical permeability

Model	Cv	Oil Recovery
10	0.44	94.7
13	0.44	96.5
18	0.54	95.7

Furthermore, Table 5. shows the recovery and Cv for the models in which both the horizontal and vertical permeability was made to vary simultaneously.

Table 5. Oil recovery for variation in both kx and kz

Model	Cv	Oil Recovery
11	0.44	63.1
14	0.44	63.8
15	0.56	84.5
16	0.28	70
20	0.79	61.5
21	0.65	65.5
22	0.34	77.6

4. Conclusions

Knowing what happens to the flow of CO_2 and hydrocarbon in the presence of fine-scale geological structures is important to determine the amount of CO_2 needed and how much hydrocarbon will be recovered. Understanding whether the flow is viscous-dominated or gravity-dominated could give some economic indications on the project and prevent the bypass of valuable oil. After running 21 models and analyzing the different outputs, the following were concluded:

1. The MMP for all models was found to be between 150 bars and 200 bars and was taken to be 175 bars. At pressures below the MMP, flow tends to be gravity-dominated and is affected mostly by gravity and less by permeability and tends to override. At pressures higher than the MMP, the oil and gas become one phase and the flow is viscous-dominated and takes the path of least resistance or highest permeability first. As a result, fingering occurs, and early breakthrough occurs in these layers.
2. All models show an increase in recovery due to miscibility. Having a k_v/k_h ratio greater than unity does not affect oil recovery and yields a similar recovery as that of the homogeneous. On the other hand, having k_v/k_h ratio less than unity affects oil recovery. As the ratio decreases, the recovery increases, with the best recovery being at k_v=0 (i.e., no cross flow).
3. Coarsening of the vertical permeability only does not have significant effect on oil recovery but the coarsening of the horizontal or both horizontal and vertical permeabilities reduces recovery greatly. Also, fining of vertical permeability does not affect oil recovery but fining of either horizontal permeability or both reduces recovery by a great amount.
4. The degree of gas override increases or decreases depending on both horizontal and vertical permeability. For example, having random permeability distribution distorts the flood front and causes fingering and the effect of gas override diminishes.
5. The variation of horizontal permeability has the most effect on oil recovery, regardless of whether vertical permeability is constant or varying as well. However, the coefficient of variation cannot be used alone as a measure of heterogeneity in CO_2 flooding, since two models with the same Cv value can yield different recoveries. No relation between Cv and recovery could be determined from the current available data.

References

Abubakar Isah, Abubakar Isah, Muhammad Arif, Muhammad Arif, Amjed Hassan, Amjed Hassan, Mohamed Mahmoud, Mohamed Mahmoud, Stefan Iglauer, and Stefan Iglauer. 2022. “A Systematic Review of Anhydrite-Bearing Reservoirs: EOR Perspective, CO2-Geo-Storage and Future Research.” *Fuel* 320 (July): 123942–123942. https://doi.org/10.1016/j.fuel.2022.123942.

Ahmed, Tarek. 2006. *Reservoir Engineering Handbook (Vol. 1)*. United States of America: Elsevier Inc.

Alvarado, Vladimir, and Eduardo Manrique. 2010. *Enhanced Oil Recovery: Field Planning and Development Strategies*. Gulf Professional Publishing.

Antolinez, Juan D., Rahman Miri, and Alireza Nouri. 2023. “In Situ Combustion: A Comprehensive Review of the Current State of Knowledge.” *Energies* 16 (17): 6306.

Ayomikun Bello, Anastasia A. Ivanova, and Alexey Cheremisin. 2023. “A Comprehensive Review of the Role of CO2 Foam EOR in the Reduction of Carbon Footprint in the Petroleum Industry.” *Energies* 16 (3): 1167–1167. https://doi.org/10.3390/en16031167.

Carcoana, Aurel. 1992. “Applied Enhanced Oil Recovery.”

Fahad I. Syed, Fahad I. Syed, Temoor Muther, Temoor Muther, Amirmasoud Kalantari Dahaghi, Amirmasoud K. Dahaghi, Shahin Neghabhan, and Shahin Neghabhan. 2022. “CO2 EOR Performance Evaluation in an Unconventional Reservoir through Mechanistic Constrained Proxy Modeling.” *Fuel* 310 (February): 122390. https://doi.org/10.1016/j.fuel.2021.122390.

Gervasio Pimenta, Gervásio Pimenta, Carolina Romero, and Carolina Romero. 2022. “CO2 EOR Challenges and Opportunities to Enable CCUS Strategies.” *Day 4 Thu, November 03, 2022*, October. https://doi.org/10.2118/211464-ms.

Holm, L. W., and V. A. Josendal. 1974. “Mechanisms of Oil Displacement by Carbon Dioxide.” *Journal of Petroleum Technology* 26 (12): 1427–38.

Jin, Lu, Steven Hawthorne, James Sorensen, Lawrence Pekot, Bethany Kurz, Steven Smith, Loreal Heebink, Volker Herdegen, Nicholas Bosshart, and José Torres. 2017. “Advancing CO2 Enhanced Oil Recovery and Storage in Unconventional Oil Play—Experimental Studies on Bakken Shales.” *Applied Energy* 208: 171–83.

Leonhard Ganzer, Leonhard Ganzer, Kurt M. Reinicke, and Kurt M. Reinicke. 2017. “Enhanced Oil Recovery,” September, 1–57. https://doi.org/10.1002/0471238961.0514080102151803.a01.pub3.

Mohamad Yousef Alklih, Mohamad Yousef Alklih, Khaled E. Al Hammadi, and Khaled E. Al Hammadi. 2019. “First CO2-EOR Project of the Middle East, Lessons Learnt and Future Plan after Two Years of Injection,” November. https://doi.org/10.2118/197274-ms.

Mohamad Yousef Alklih, Mohamad Yousef Alklih, Nidhal Mohamed Aljneibi, Nidhal Mohamed Aljneibi, Karem Alejandra Khan, Karem Alejandra Khan, Melike Dilsiz, and Melike Dilsiz. 2021. “Does Miscibility Alone Predict the Success of WAG Projects? Key Issues in Miscible HC-WAG Injection,” September. https://doi.org/10.2118/206116-ms.

Mostafa Iravani, Zahra Khalilnezhad, and Ali Khalilnezhad. 2023. “A Review on Application of Nanoparticles for EOR Purposes: History and Current Challenges.” *Journal of Petroleum Exploration and Production Technology* 13 (4): 959–94. https://doi.org/10.1007/s13202-022-01606-x.

Muataz Alshuaibi, Muataz Alshuaibi, Seyed Amir Farzaneh, Seyed Amir Farzaneh, Mehran Sohrabi, and Mehran Sohrabi. 2018. “An Experimental and Simulation Investigation on the Effect of Different Gas Mixtures on Performance of Miscible CO2 Injection in HPHT Abu Dhabi Reservoir,” September. https://doi.org/10.2118/191496-ms.

Pan, Yi, Wei Qiao, Dexia Chi, Zhaoxuan Li, and Yunjie Shu. 2023. “Research of Steam Injection In-Situ Production Technology to Enhance Unconventional Oil and Gas Recovery: A Review.” *Journal of Analytical and Applied Pyrolysis*, 106332.

Pashapouryeganeh, Farzad, Ghasem Zargar, Ali Kadkhodaie, Ahmad Rabiee, Ali Misaghi, and Seyed Jamal Sheikh Zakariaei. 2022. “Experimental Evaluation of Designed and Synthesized Alkaline-Surfactant-Polymer (ASP) for Chemical Flooding in Carbonate Reservoirs.” *Fuel* 321: 124090.

Ragab, Ahmed, and Eman M. Mansour. 2021. “Enhanced Oil Recovery: Chemical Flooding.” *Geophysics and Ocean Waves Studies* 51.

Razman Shah, Nur Batrisyia Bt, Rozana Azrina Bt Sazali, Kenneth Stuart Sorbie, Munawar Khalil, and Azlinda Azizi. 2023. “Nanomaterials for Scaling Prevention in Alkaline–Surfactant–Polymer Flooding: A Review.” *Applied Nanoscience* 13 (6): 3945–74.

Seyedeh Hosna Talebian, Seyedeh Hosna Talebian, Rahim Masoudi, Rahim Masoudi, Isa M. Tan, Isa M. Tan, Pacelli L.J. Zitha, Pacelli L.J. Zitha, and Pacelli L.J. Zitha. 2014. “Foam Assisted CO2-EOR: A Review of Concept, Challenges, and Future Prospects.” *Journal of Petroleum Science and Engineering* 120 (August): 202–15. https://doi.org/10.1016/j.petrol.2014.05.013.

Xiao Deng, Xiao Deng, Zeeshan Tariq, Zeeshan Tariq, Mobeen Murtaza, Mobeen Murtaza, Shirish Patil, et al. 2020. “Relative Contribution of Wettability Alteration and Interfacial Tension Reduction in EOR: A Critical Review.” *Journal of Molecular Liquids* 325: 115175. https://doi.org/10.1016/j.molliq.2020.115175.

Zhao, Fang, Changfeng Xi, Xialin Zhang, Xiao Rong Shi, Fengxiang Yang, Hetaer Mu, Wenlong Guan, Hongzhuang Wang, Hongyang Zhan, and Tayfun Babadagli. 2021. “Analysis on the Main Influential Factors of Post-Steam In-Situ Combustion Performance in Heavy Oil Reservoir.” *Journal of the Japan Petroleum Institute* 64 (2): 76–83.

Zhao, Fang, Changfeng Xi, Xialin Zhang, XiaoRong Shi, Fengxiang Yang, Hetaer Mu, Wenlong Guan, Youwei Jiang, Hongzhuang Wang, and Tayfun Babadagli. 2020. “Evaluation of a Field-Wide Post-Steam In-Situ Combustion Performance in a Heavy Oil Reservoir in China.” In *SPE Russian Petroleum Technology Conference*. OnePetro.

Zhengxiao Xu, Xu Zhengxiao, Guohe Huang, Song-Yan Li, Songyan Li, Binfei Li, Binfei Li, et al. 2020. “A Review of Development Methods and EOR Technologies for Carbonate Reservoirs.” *Petroleum Science* 17 (4): 990–1013. https://doi.org/10.1007/s12182-020-00467-5.

Appendix A

Table A.1: Component Fluid Properties

Component	Critical Temperature (K)	Critical Pressure (bars)	Acentric Factor	Molecular Weights	Boiling Points (K)	Initial oil Composition
CO2	304.2	72.80	0.225	44.010	194.7	0.0118
N2-CH4	189.67	45.24	0.0084	16.208	113.656	0.1170
C2-NC4	338.44	41.92	0.1481	44.793	259.432	0.1945
IC5-C7	556.92	31.31	0.2485	83.458	340.618	0.2202
C8-C12	667.51	23.86	0.3279	120.524	415.671	0.2815
C13-C19	769.00	17.23	0.5672	210.743	543.642	0.0940
C20-C30	801.51	11.9	0.9422	401.926	735.01	0.0809

Table A.2: Reservoir Properties

Parameter	Value	Units
Porosity	0.1	-
Permeability in the x-direction	500	mD
Permeability in the z-direction	500	mD
Rock Compressibility	$5x10^{-5}$	$Bars^{-1}$
Temperature	53	C
Capillary Pressure	0	Bars
Wellbore Diameter	0.02	m
CO_2 injection rate	0.48	m^3/day

Table A.3: Relative permeability data

Sg	Krg	Krog	Pc
0	0	1	0
0.02	0	1	0
0.045	9.21E-05	0.8538	0
00.07	0.000642	0.7233	0
0.095	0.002	0.6076	0
0.12	0.0045	0.5056	0
0.145	0.0084	0.4164	0
0.17	0.0139	0.3388	0
0.195	0.0214	0.2721	0
0.22	0.0312	0.2152	0
0.245	0.0433	0.1673	0
0.27	0.0582	0.1275	0
0.295	0.076	0.0948	0
0.32	0.097	0.0686	0
0.345	0.1214	0.048	0
0.37	0.1494	0.0321	0
0.395	0.1813	0.0204	0
0.42	0.2172	0.0121	0
0.445	0.2574	0.0065	0
0.47	0.302	3.05E-03	0
0.495	0.3514	1.15E-03	0
0.52	0.4057	2.89E-04	0
0.545	0.4651	0	0
0.57	0.5298	0	0
0.595	0.6001	0	0
0.62	0.6761	0	0
0.645	0.758	0	0
0.67	0.846	0	0
0.71	1	0	0
0.77	1	0	0
0.83	1	0	0

Table A.4 Permeability distribution for models 2-4

Model no.	Horizontal permeability (mD)	Vertical permeability (mD)	Kv/kh ratio
2	125	500	4
3	250	500	2
4	375	500	1.333

Table A.5: Permeability distribution for models 5-7

Model no.	Horizontal permeability (mD)	Vertical permeability (mD)	Kv/kh ratio
5	500	125	0.25
6	500	250	0.5
7	500	375	0.75

Table A.6: Permeability distribution for model 8

Layer no.	Horizontal Permeability (mD)	Vertical Permeability (mD)
1	500	500
2	450	500
3	400	500
4	350	500
5	300	500
6	250	500
7	200	500
8	150	500
9	100	500
10	50	500

Table A.7: Permeability distribution for model 9

Layer no.	Horizontal Permeability (mD)	Vertical Permeability (mD)
1	500	500
2	500	450
3	500	400
4	500	350
5	500	300
6	500	250
7	500	200
8	500	150
9	500	100
10	500	50

Table A.8: Permeability distribution for model 10

Layer no.	Horizontal Permeability (mD)	Vertical Permeability (mD)
1	500	500
2	450	450
3	400	400
4	350	350
5	300	300
6	250	250
7	200	200
8	150	150
9	100	100
10	50	50

Table A.9: Permeability distribution for model 11

Layer no.	Horizontal Permeability (mD)	Vertical Permeability (mD)
1	50	500
2	100	500
3	150	500
4	200	500
5	250	500
6	300	500
7	350	500
8	400	500
9	450	500
10	500	500

Table A.10: Permeability distribution for model 12

Layer no.	Horizontal Permeability (mD)	Vertical Permeability (mD)
1	500	50
2	500	100
3	500	150
4	500	200
5	500	250
6	500	300
7	500	350
8	500	400
9	500	450
10	500	500

Table A.11: Permeability distribution for model 13

Layer no.	Horizontal Permeability (mD)	Vertical Permeability (mD)
1	50	50
2	100	100
3	150	150
4	200	200
5	250	250
6	300	300
7	350	350
8	400	400
9	450	450
10	500	500

Table A.12: Permeability distribution for model 14

Layer no.	Horizontal Permeability (mD)	Vertical Permeability (mD)
1	500	500
2	100	100
3	500	500
4	100	100
5	500	500
6	100	100
7	500	500
8	100	100
9	500	500
10	100	100

Table A.13: Permeability distribution for model 15

Layer no.	Horizontal Permeability (mD)	Vertical Permeability (mD)
1	500	500
2	250	250
3	500	500
4	250	250
5	500	500
6	250	250
7	500	500
8	250	250
9	500	500
10	250	250

Table A.14: Permeability distribution for model 16

Layer no.	Horizontal Permeability (mD)	Vertical Permeability (mD)
1	150	500
2	300	500
3	50	500
4	200	500
5	100	500
6	200	500
7	400	500
8	250	500
9	50	500
10	500	500

Table A.15: Permeability distribution for model 17

Layer no.	Horizontal Permeability (mD)	Vertical Permeability (mD)
1	500	150
2	500	300
3	500	50
4	500	200
5	500	100
6	500	200
7	500	400
8	500	250
9	500	50
10	500	500

Table A.16: Permeability distribution for model 18

Layer no.	Horizontal Permeability (mD)	Vertical Permeability (mD)
1	500	500
2	200	500
3	65	500
4	250	500
5	180	500
6	10	500
7	800	500
8	150	500
9	60	500
10	200	500

Table A.17: Permeability distribution for model 19

Layer no.	Horizontal Permeability (mD)	Vertical Permeability (mD)
1	500	500
2	200	200
3	65	65
4	250	250
5	180	180
6	10	10
7	800	800
8	150	150
9	60	60
10	200	200

Table A.18: Permeability distribution for model 20

Layer no.	Horizontal Permeability (mD)	Vertical Permeability (mD)
1	46	46
2	656	656
3	200	200
4	365	365
5	789	789
6	365	365
7	62	62
8	200	200
9	652	652
10	50	50

Table A.19: Permeability distribution for model 21

Layer no.	Horizontal Permeability (mD)	Vertical Permeability (mD)
1	250	250
2	220	220
3	500	500
4	320	320
5	700	700
6	400	400
7	200	200
8	300	300
9	500	500
10	600	600